processes

MDPI

Article

Comparison of CBM Productivity with Hydraulic Fracturing, Slotting, and Cavity Creation in Cleat–Developed Coal Seams

Haibing Lu [1,2], Jiaxiang Xu [3,*], Yuhang Xiao [1,2], Meizhu Wang [1,2], Xueying Zhang [1,2], Wanxin Fu [3] and Xingyuan Zhu [3]

[1] Research Institute of Petroleum Exploration and Development, Beijing 100083, China; luhaibing69@petrochina.com.cn (H.L.); yjy_xyh@petrochina.com.cn (Y.X.); wangmeizhu69@petrochina.com.cn (M.W.); yjzx_zxying@petrochina.com.cn (X.Z.)
[2] Coalbed Methane Key Laboratory of China National Petroleum Corporation, Beijing 100083, China
[3] College of Petroleum Engineering, Liaoning Petrochemical University, Fushun 113001, China; wanxin_0618@126.com (W.F.); xingyuan_4616@126.com (X.Z.)
* Correspondence: shigong101121@163.com

Abstract

Hydraulic fracturing, slotting, and cavity creation are commonly employed techniques to enhance coalbed methane (CBM) development. To investigate the applicability of these three stimulation methods, this study proposes a mathematical method for constructing coal seams with orthogonal cleats, and integrates it with hydraulic fracturing, slotting, and cavity creation to generate three coal seam stimulation models. Considering desorption and diffusion of adsorbed gas, a coupled flow model of CBM in the coal matrix–cleat–hydraulic fracture/slot/cavity system was established. The results indicate that among the three stimulation methods, the stable production period and peak production resulting from slotting are less sensitive to cleat density, enhancing its applicability across diverse coal seams. Hydraulic fracturing yields a higher peak daily production than slotting, reaching 411 m^3/d, but its stable production period is shorter, averaging 7.2 years, and its cumulative production is slightly lower than that of slotting when the cleat density is low. In coal seams with low cleat density, the stable production period and cumulative production of the cavity are inferior to those of hydraulic fracturing and slotting. However, when the cleat density is high, the production of cavity creation can reach the levels of hydraulic fracturing and slotting, with cumulative production of 78 × 10^4 m^3.

Keywords: coalbed methane; hydraulic fracturing; slotting; cavity creation; productivity simulation

check for updates

Academic Editor: Qingbang Meng

Received: 24 August 2025
Revised: 4 October 2025
Accepted: 9 October 2025
Published: 10 October 2025

Citation: Lu, H.; Xu, J.; Xiao, Y.; Wang, M.; Zhang, X.; Fu, W.; Zhu, X. Comparison of CBM Productivity with Hydraulic Fracturing, Slotting, and Cavity Creation in Cleat–Developed Coal Seams. *Processes* **2025**, *13*, 3228. https://doi.org/10.3390/pr13103228

Copyright: © 2025 by the authors. Licensee MDPI, Basel, Switzerland. This article is an open access article distributed under the terms and conditions of the Creative Commons Attribution (CC BY) license (https://creativecommons.org/licenses/by/4.0/).

1. Introduction

Coalbed methane (CBM), as an unconventional natural gas resource, serves as a significant supplement to global clean energy resources. It is abundantly available and primarily distributed in the Appalachian Basin and Powder River Basin in the United States, the Alberta Basin in Canada, and the Qinshui Basin and Ordos Basin in China [1–5]. The main component of CBM is methane, which burns cleanly and has a high calorific value. This dual benefit of greenhouse gas reduction and energy supply endows CBM with substantial potential for utilization [6–8]. Furthermore, the geological and geomechanical characteristics of coal seams, such as their rock mechanical properties and time–dependent behavior, are highly basin–specific and play a critical role in determining optimal recovery strategies [9].

However, the current development of CBM faces numerous technical and economic challenges. Firstly, CBM is stored in the micropores and fractures of coal seams, typically in an adsorbed state, which results in complex occurrence conditions, poor reservoir properties, and low permeability, leading to inefficient gas desorption and migration [10–13]. This issue is exacerbated in deep, high–stress coal seams, where limited fracture development and pronounced pressure sensitivity further hinder extraction [14,15]. Consequently, reservoir stimulation technologies aimed at enhancing the recovery of CBM and improving single–well production have been developed, including large–scale hydraulic fracturing, foam fracturing, and pulse fracturing [16–21]. Hydraulic fractures combining cleats provide important permeability pathways within coal seams, greatly influencing the extraction of gases and fluids. Cleats are crucial in coal bed methane production as they allow gas to move through the coal and be extracted. Cleats in coal seams are natural, regularly spaced fractures or joints that develop within coal beds. There are face cleats and butt cleats. Face cleats are the dominant, continuous fractures running in one direction. Butt cleats are discontinuous fractures that usually intersect the face cleats at approximately right angles.

After reservoir stimulation, the production of CBM wells typically declines rapidly over time. Consequently, researchers have conducted extensive studies on the changes in productivity of fractured CBM wells, focusing on aspects such as coal seam structure, gas–water relationships, and fracturing techniques [18–23]. These studies emphasize analyzing the key factors influencing CBM productivity using the theory of two–phase gas–water flow. Zhang [24] developed a three–dimensional dual–porosity two–phase flow numerical model based on petroleum geology and flow mechanics, combined with tests from western CBM fields. Jiang et al. [25] established a gas–water two–phase flow model for CBM wells based on the Buckley–Leverett equation, which emphasized three main control factors: matrix gas supply capacity, fracture conductivity, and main fracture drainage capacity. Zhu et al. [26] constructed a gas–water two–phase flow model considering the differences in stress sensitivity between hydraulic fractures and the reservoir. Chen et al. [27] analyzed five factors, including differential in situ stress, affecting the fracturing effect in the Qinshui Basin. A classification evaluation model was established using a support vector machine, concluding that a small stress differential, large fracture volume, and complex fracture morphology are beneficial for productivity enhancement.

In addition to establishing high–conductivity channels within coal seams through fracturing, techniques such as slotting or cavity creation can be employed to reduce coal seam stress and enhance permeability [28–30]. The cavity creation method was developed for CBM extraction in the San Juan Basin in 1985 [31–33]. CBM wells completed using this method exhibited gas productivity nearly ten times greater than that of hydraulically fractured vertical wells. Shi et al. [34] conducted a numerical simulation of CBM cavity wells in the San Juan Basin using a geomechanical finite element model, demonstrating that formation permeability is the most critical factor controlling cavity well productivity. Wei et al. [35] systematically analyzed microstructural changes and permeability enhancement using hydraulic slotting and liquid CO_2 injection. They found that the porosity and permeability of the coal increased by 47.65% and 65.31%, respectively, with a CH_4 recovery rate exceeding 90%, and the residual gas content in the coal seam reducing to 8.0 m^3/t. Lin et al. [36] demonstrated that borehole hydraulic slotting technology significantly enhances the efficiency of gas extraction in coal mine roadways, with the influence range of slotted holes being 12.87 times that of conventional holes and gas concentration increasing to 3.7 times its original level. Si et al. [37] systematically analyzed the impact of various geological and process parameters (such as in situ stress, slot geometry, spacing, etc.) on the volume of the damage zone induced by slotting, clarifying the order of the main controlling parameters affecting slotting effectiveness. Chen et al. [38] revealed that

the total CBM production after slotting is 4.41 times those under traditional completion, suggesting that slotting can effectively enhance CBM productivity. Qin et al. [39] also confirmed that hydraulic slotting significantly increased CBM extraction. Zhen et al. [40] demonstrated strategically induced cavity elevated fluid pressures in stress–concentrated areas, effectively neutralizing compressive stresses and restoring reservoir permeability.

However, hydraulic fracturing, slotting and cavity creation has been proved to work only under specific reservoir, geological, and geo–mechanical conditions due to the mechanism differences in these three stimulation methods. Therefore, a coupled flow model of CBM in the coal matrix–cleat–hydraulic fracture/slot/cavity creation system was established and utilized in the cleat–developed coal seam model to real their applications.

2. Coal Seam Stimulation Models

The coal seam stimulation model established in this study comprises two components: the coal seam and the stimulated region. The coal seam consists of the matrix, face cleats, and butt cleats, where the face cleats are randomly distributed along the thickness direction of the coal seam, and the butt cleats are randomly distributed between two adjacent face cleats, orthogonal to the face cleats. The flow chart of coal seam construction is presented in Figure 1. The stimulated region is located at the center of the coal seam's end face and is categorized into three schemes: hydraulic fracturing (represented by a single elongated cuboid), slotting (represented by multiple small rectangular prisms), and cavity creation (represented by a cylinder bisected axially), presented in Figure 2. The specific geometric parameters of the coal seam region and the stimulated region are detailed in Tables 1 and 2. In real coal seams, cleats and fractures are rough, and cavities are not perfect cylinders. In this research, these are simplified by assuming that cleats and fractures are regular and smooth planes, and cavities are cylindrical. This approach is due in part to the inability to obtain real and accurate shapes of cleats, fractures, and cavities in the field and also because it significantly reduces the computational load of numerical simulations while ensuring reliable accuracy.

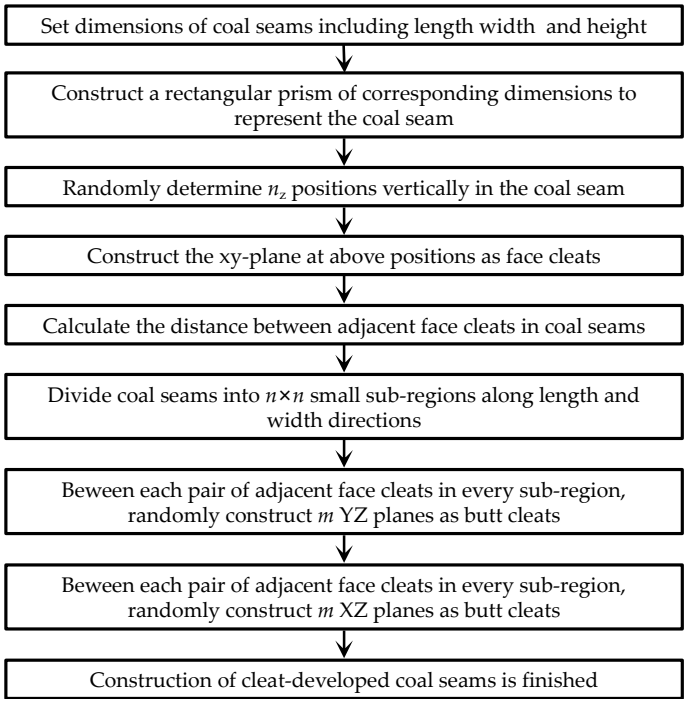


Figure 1. Flow chart of coal seam model construction.

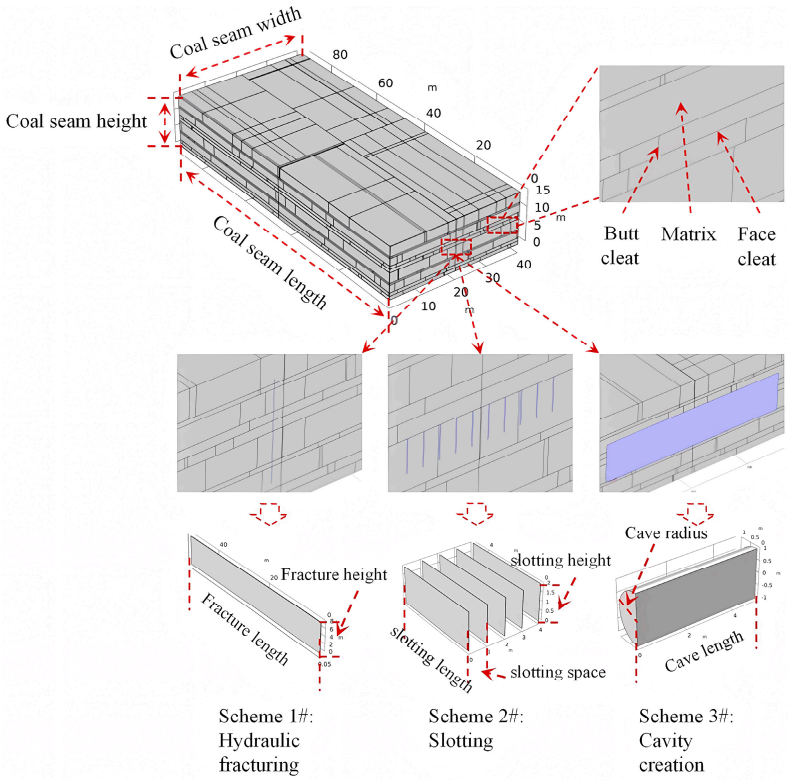


Figure 2. Three different stimulation methods in coal seam.

Table 1. Geometrical parameters of coal seams.

Coal Seam Length (m)	Coal Seam Width (m)	Coal Seam Height (m)	Number of Face Cleats	Number of Butt Cleats	Coal Seam Name
90	40	15	3	16	Coal seam 1#
			5	96	Coal seam 2#
			7	168	Coal seam 3#
			9	320	Coal seam 4#

Table 2. Geometry parameters of different stimulation methods in coal seam.

Stimulation Methods	Length (m)	Width (mm)	Height (m)	Radius (m)	Number	Space (m)
Hydraulic fracturing	50/60/70	10	10	–	1	–
Slotting	5	5	2	–	5/10/15	1
Cavity creation	5/10/15/20/25/30	–	–	0.5/1.0/1.5/2.0/2.5/3.0	1	–

This method allows for controlling the density of the coal seams' butt cleats and face cleats by adjusting the number of xy, xz, and yz planes within the model. By adjusting the number of sub–regions, the connectivity of the cleats can be controlled, making it a new method for constructing arbitrary orthogonal face cleats and butt cleats at the coal seam scale. However, this method can only construct orthogonal cleats with the assumption that the cleats are regular planes, and it cannot represent the diversity of angles between cleats or the roughness of cleat surfaces in the real coal seam. Depending on the scale of the constructed coal seam, this method can be used to construct coal rock and the cleats within it at the core scale to analyze the flow characteristics of coalbed methane, or it can construct large–scale coal seams and the cleats within them to analyze the changes in coalbed methane productivity under different stimulation methods.

3. Development Model of CBM

Generally, CBM exists in the coal seam in three forms: adsorbed, free, and dissolved. During the development of CBM, the process involves the extraction of free gas and the desorption and diffusion of adsorbed gas through pressure reduction. The desorption process of the adsorbed gas is characterized by the Langmuir isotherm. Consequently, the continuity equation for the seepage of CBM in the coal seam matrix can be expressed as follows [41]:

$$\frac{\partial(\rho_{cm}\phi_m)}{\partial t} + \frac{\partial\left(\rho_{st}\rho_c\frac{V_L p}{P_L + p}\right)}{\partial t} + \nabla\cdot\left(\rho_{cm}u_{gm}\right) = Q_{gm} \tag{1}$$

where ρ_{cm} is the CBM density, kg/m^3; ρ_{st} is the gas density under standard atmospheric pressure, kg/m^3; ρ_c is the density of the coal seam, kg/m^3; ϕ_m denotes the porosity of the coal seam; V_L is the Langmuir volume constant, m^3/kg; P_L is the Langmuir pressure constant, Pa; p is the reservoir pressure, Pa; u_{gm} is the gas seepage velocity in the coal matrix, m/s; Q_{gm} is the mass source/sink term in the coal matrix, kg/s.

Taking gravity into account, the motion equation of CBM within the coal matrix is expressed as:

$$u_{gm} = -\frac{k_m}{\mu_g}(\nabla p + \rho_{cm} g \nabla H) \tag{2}$$

where k_m is the permeability of the coal matrix, m^2; μ_g is the dynamic viscosity of the CBM, Pa·s; g is the gravitational acceleration, m/s^2; and H is the depth of the CBM, m. From Equations (1) and (2), the mass conservation equation for CBM within the coal matrix is derived as [41]:

$$\left[\phi_m + \frac{\rho_c p_{st} V_L P_L}{(p + P_L^2)}\right]\frac{\partial p}{\partial t} + p\frac{\partial \phi_m}{\partial t} - \nabla\left(\frac{k_m}{\mu_g}(\nabla p + \rho_{cm} g \nabla H)\right) = Q_{gm} \tag{3}$$

where p_{st} is the standard atmospheric pressure, Pa.

Treating cleats, slots, and hydraulic fractures as fractures, the continuity equation for CBM seepage in these features can be represented as:

$$\frac{\partial(d_f \phi_f \rho_{cm})}{\partial t} + \nabla\cdot\left(d_f \rho_{cm} u_{gf}\right) = d_f Q_{gf} \tag{4}$$

where d_f is the width of the cleat, slot, or fracture, m; ϕ_f is the porosity of these features; u_{gf} is the CBM seepage velocity in the cleats, slots, and hydraulic fractures, m/s; Q_{gf} is the mass source/sink term, kg/s.

The motion equation for CBM in cleats, slots, or hydraulic fractures is expressed as:

$$u_{gf} = -\frac{k_f}{\mu_g}\nabla p \tag{5}$$

where k_f is the permeability of the cleat, slot, or fracture, m^2.

The flowing of CBM in cavities is simulated using the Navier–Stokes equation, represented as follows:

$$\frac{\partial \rho_{cm} u_{gc}}{\partial t} + \rho_{cm}(u_{gc}\cdot\nabla)u_{gc} = \nabla\cdot\left[-p + \mu_g\left(\nabla u_{gc} + (\nabla u_{gc})^T\right)\right] \tag{6}$$

where u_{gc} is the CBM flow velocity in the cavity, m/s.

Due to the high compressibility of CBM, its density changes significantly during development, and the relationship between density and pressure is given by:

$$\rho_{cm} = \frac{M_g}{RT} p \tag{7}$$

where M_g represents the molar mass of the gas, g/mol; R is the gas constant, J/(mol·K); T is the temperature of the CBM, K.

Considering the effective stress and matrix shrinkage effects of the coal seam, the stress sensitivity models for porosity and permeability of the coal matrix are described, respectively, as:

$$\phi_m = \phi_{m0} + \lambda_m(p - p_0) + \varepsilon_l\left(\frac{K}{M} - 1\right)\left(\frac{\zeta p}{1+\zeta p} - \frac{\zeta p_0}{1+\zeta p_0}\right) \tag{8}$$

$$k_m = k_{m0}\left(\frac{\phi_m}{\phi_{m0}}\right)^3 \tag{9}$$

where $\lambda_m = \frac{1}{M} - \left(\frac{K}{M} + f - 1\right)\gamma$, $\frac{K}{M} = \frac{1}{3}\left(\frac{1+v}{1-v}\right)$, $\zeta = \frac{1}{P_L}$, ϕ_{m0} is the initial porosity of the coal seam; p_0 is the initial pressure of the coal seam, Pa; ε_l is the Langmuir volume strain constant; K is the bulk modulus of the coal, Pa; M is the uniaxial modulus of the coal, MPa; f ranges from 0 to 1; γ is the coal particle compressive coefficient, Pa^{-1}; k_{m0} is the initial permeability of the coal seam, m^2; v is Poisson's ratio.

The stress sensitivity of cleats, slots, or hydraulic fractures in the coal seam can be expressed as:

$$k_f = k_{f0}e^{-\beta\sigma} \tag{10}$$

where k_{f0} is the initial permeability of the cleat, slot, or hydraulic fracture, m^2; σ represents the effective stress on the coal seam from the initial state to a test point, Pa; β is the stress sensitivity coefficient of the cleat, slot, or hydraulic fracture, Pa^{-1}.

To validate the accuracy of the model, numerical calculations were conducted using the physical and stimulation characteristics of well JH11–8 in the FJ CBM field, and the results were compared with the actual gas production from the well, as shown in Figure 3. The parameters employed in the calculation are provided in Table 3. It can be observed that the trend of daily production obtained from numerical simulation is in good agreement with the actual production data, with a cumulative production error of 4.74%, indicating a certain level of accuracy in the model.

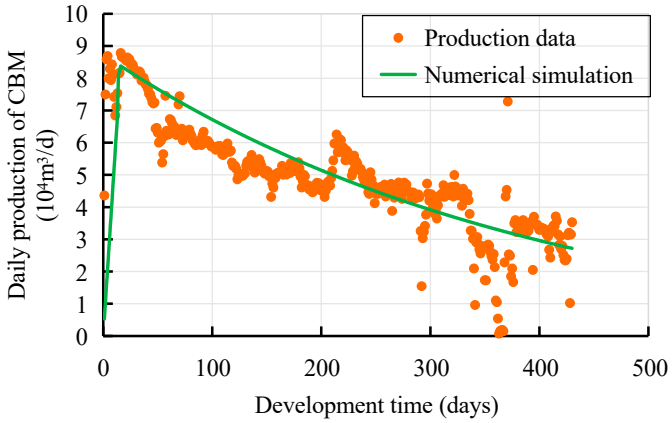


Figure 3. Comparison of numerical simulation and real production data.

Table 3. Physical parameter of Well JH11–8.

Parameters	Value	Parameters	Value
Coal seam depth (m)	2185	Cleats width (mm)	1.4
Coal seam thickness (m)	7.8	Matrix permeability (10^{-3} μm^2)	0.09
Coal seam porosity (%)	3.69	Langmuir volume constant (m^3/t)	25.3
Density of face cleats (1/m)	60–240	Langmuir pressure constant (MPa)	2.87
Density of butt cleats (1/m)	40–200	Poisson's ratio of coal seam	0.38
Fracture length (m)	78	Young's modulus of coal seam (GPa)	4.5
Fracture width (mm)	3.5	Bulk modulus of coal seam (GPa)	6.5
Fracture height (m)	7.68	Reservoir pressure coefficient	0.93
Fracture permeability (μm^2)	12	Gas saturation (%)	93.6

In further simulation of post–enhancement CBM productivity using the aforementioned model, the required simulation parameters were set based on previous numerical simulations and surveys of typical blocks [42–44], as shown in Table 4.

Table 4. Parameters in simulation.

Parameters	Value	Unit
Coal seam depth	1800	m
Coal seam density	1520	kg·m^{-3}
Initial porosity of coal seam	0.1	–
Initial permeability of coal seam	0.01	10^{-3} μm^2
Initial permeability of cleats in coal seam	10	10^{-3} μm^2
Initial permeability of hydraulic fractures	10	μm^2
Initial permeability of slotting	1	μm^2
Initial pressure in coal seam	20	MPa
CBM density at standard atmospheric pressure	0.716	kg·m^{-3}
Langmuir volume constant	35	m^3·t^{-1}
Langmuir pressure constant	2.5	MPa
Langmuir volumetric strain constant	0.03	–
Molar mass of CBM	16	g·mol^{-1}
Dynamic viscosity of CBM	1.65	10^{-5} Pa·s
Bulk modulus of coal seam	1000	MPa
Poisson's ratio of coal seam	0.26	–
Cleat stress sensitivity coefficient	0.45	–
Slotting stress sensitivity coefficient	0.48	–
Fracture stress sensitivity coefficient	0.50	–
Biot coefficient	0.93	–

4. Simulation Results

Taking the development of CBM via slotting as an example, the simulation results show pressure variations in coal seams with developed cleats, as illustrated in Figure 4. The results indicate that as the development pressure in the slotting decreases, the pressure within the cleats initially drops, segmenting the coal seam into high–pressure zones of varying sizes, with the low–pressure zones advancing from the cleats into the coal matrix. The minimum pressure values within the coal seam (represented by downward triangles in the legends of subplots in Figure 4) are located in the cleats near the slotting, while the maximum pressure values (represented by upward triangles in the legends of subplots in Figure 4) are found within the coal matrix. Specifically, the minimum pressure decreases from 16.4 MPa in the first year of development to 1.2 MPa in the fifteenth year, driving the maximum pressure in the matrix from 18.7 MPa to 11 MPa over the same period. However, in the early stages of development, the pressure in the cleats drops more rapidly, causing a

pressure differential increase to 10.4 MPa by the eleventh year. Subsequently, the pressure in the cleats stabilizes while the matrix pressure decreases steadily, reducing the pressure differential to 9.8 MPa by the fifteenth year. The post–hydraulic fracturing and cavity creation pressure distributions within the coal seam are similar to those by slotting, with the variations in their maximum pressure Pmax, minimum pressure Pmin, and pressure difference depicted in Figure 5.

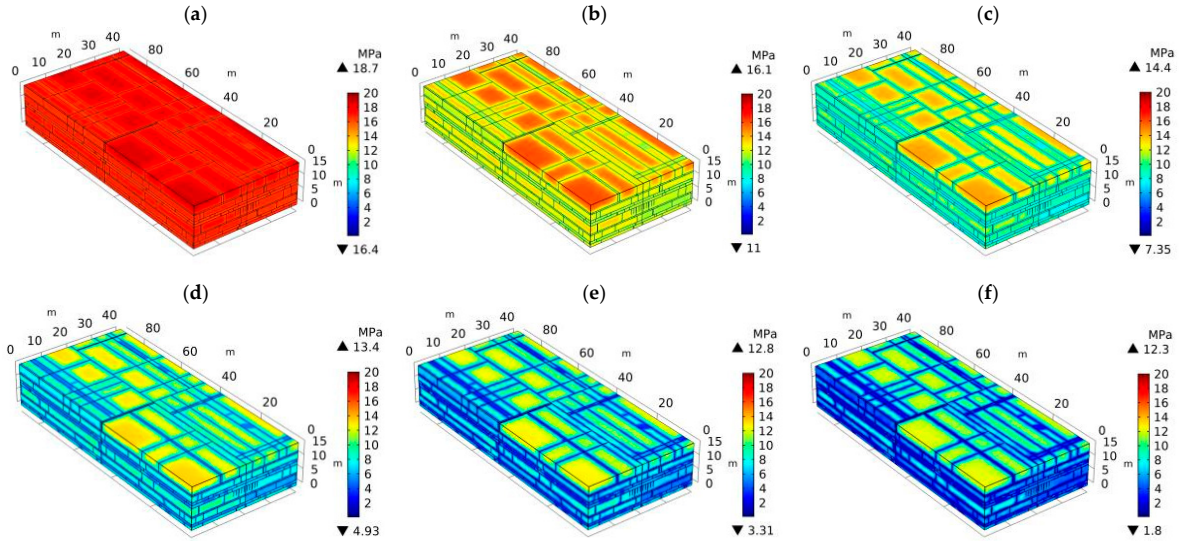


Figure 4. Pressure dynamic variation in cleat–developed coal seam at different development times: (**a**) Development time is 1 year; (**b**) Development time is 3 years; (**c**) Development time is 5 years; (**d**) Development time is 7 years; (**e**) Development time is 9 years; (**f**) Development time is 11 years.

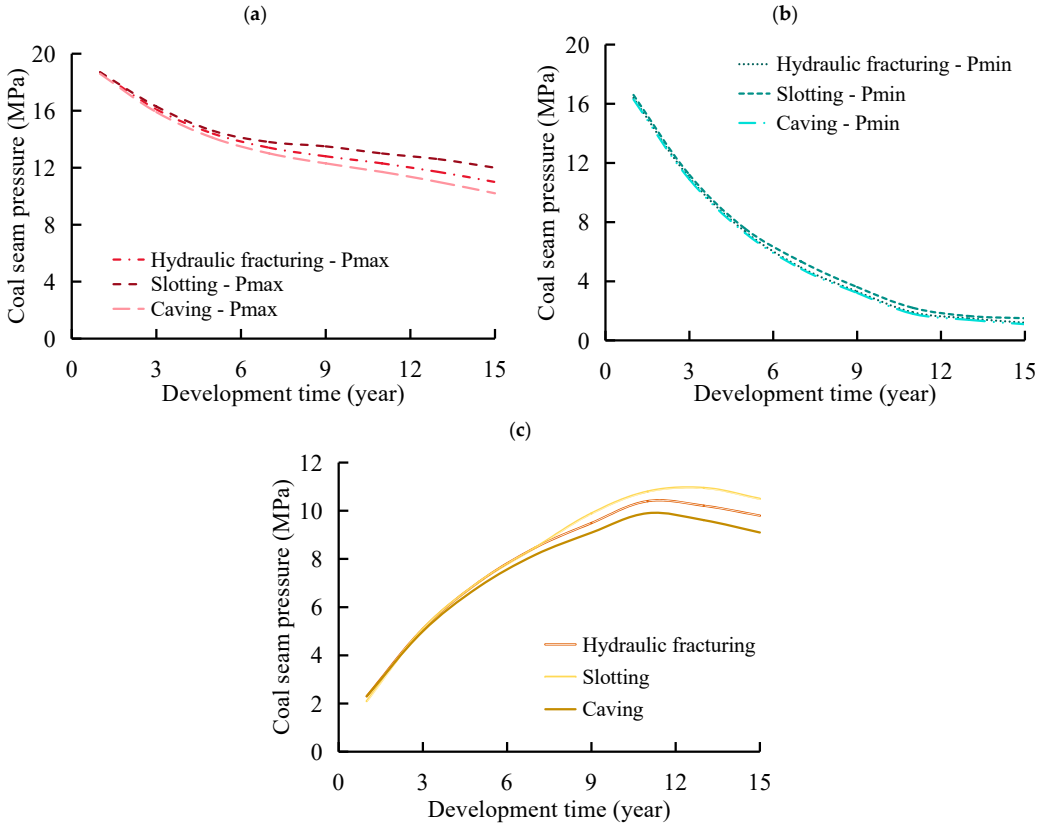


Figure 5. Variation in pressure extreme value in cleat–developed coal seam: (**a**) Maximum pressure; (**b**) Minimum pressure; (**c**) Pressure difference.

4.1. Effects of Fracture Length on CBM Productivity

For cleat–developed coal seams developed using hydraulic fracturing, the simulation results illustrating the impact of fracture length on CBM daily production are presented in Figure 6. The results indicate that with an increase in the number of cleats in Coal seam #1, Coal seam #2, Coal seam #3, and Coal seam #4, the peak production of fractures with different lengths increases. Moreover, within the same coal seam, the peak production of fractures also rises with an increase in fracture length. However, compared to fracture length, the number of cleats within the coal seam has a more significant impact on production. Specifically, the peak production of fractures in Coal seam #1 coal seam ranges from 282 m^3/d to 318 m^3/d, whereas in Coal seam #4, the peak production increases to 395 m^3/d to 411 m^3/d. When the number of cleats within the coal seam is relatively low, the peak production of fractures typically occurs around 0.5 years development. In contrast, when the number of cleats increases to that of Coal seam #4, the peak production of fractures appears after 1 year of development.

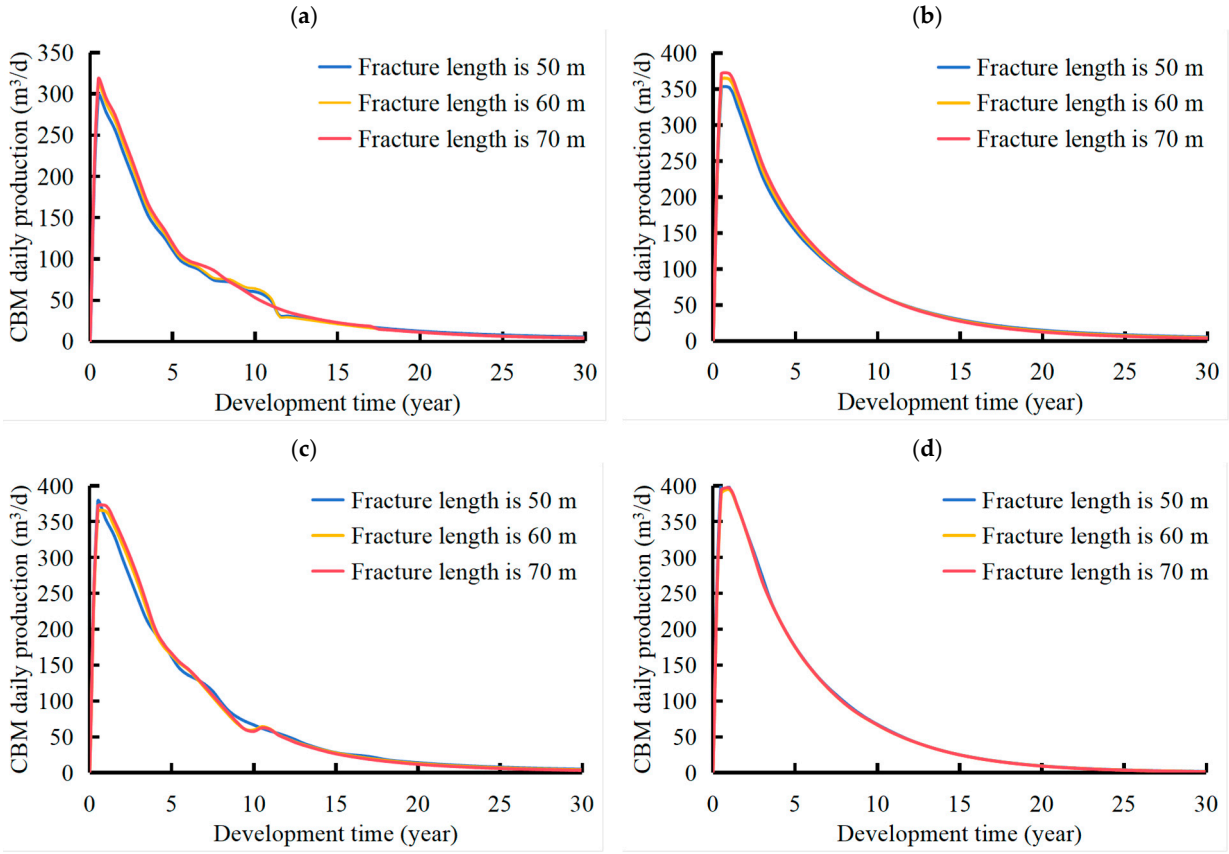


Figure 6. Effects of fracture length on productivity in different coal seams: (**a**) Coal seam 1#; (**b**) Coal seam 2#; (**c**) Coal seam 3#; (**d**) Coal seam 4#.

4.2. Effects of Slot Number on CBM Productivity

When developing cleat–developed CBM through slotting, the simulation results illustrating the impact of the number of slottings on CBM daily production are shown in Figure 7. Similarly, the peak production of CBM increases with the number of cleats in the four different coal seams. Notably, when the number of cleats in the coal seam exceeds that of Coal seam #2, the effect of cleat quantity on the enhancement of peak CBM production becomes more pronounced compared to the number of fractures. In Coal seam #2, the peak productions for low, medium, and high cleat densities are 303 m^3/d, 337 m^3/d, and 355 m^3/d, respectively, whereas in Coal seam #4, these values are 315 m^3/d, 357 m^3/d, and 381 m^3/d, respectively. Additionally, the time to reach peak daily production for the three

slotting densities in Coal seam #1 is 1.5 years, for Coal seam #2 it is either 1.5 or 1 year, and for Coal seam #3 and Coal seam #4 it is 1 year. This indicates that when using slotting for development, the time to attain peak daily production decreases as the number of slotting increases.

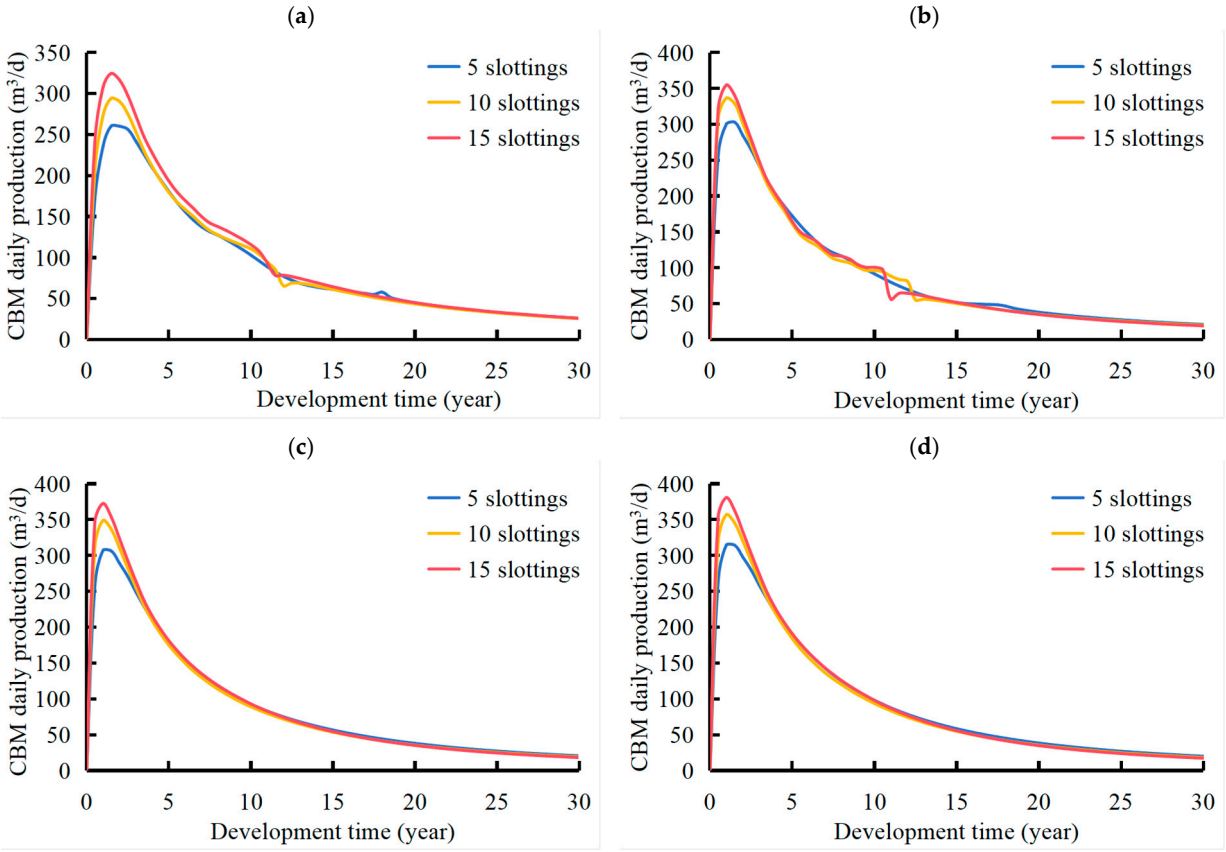


Figure 7. Effects of slot number on productivity in different seams: (**a**) Coal seam 1#; (**b**) Coal seam 2#; (**c**) Coal seam 3#; (**d**) Coal seam 4#.

4.3. Effects of Cave Length on CBM Productivity

When developing cleat–developed CBM through cavity creation, the simulation results illustrating the impact of cave length on CBM production are depicted in Figure 8. Similarly to the effects of hydraulic fracture length and cleat quantity, in coal seams with a higher number of cleats, the peak daily production for cavities of various lengths is enhanced. Moreover, as the number of cleats in the coal seam increases, the magnitude of peak daily production improvement also increases. For instance, for a cave length of 10 m, the peak daily production in Coal seam #2, Coal seam #3, and Coal seam #4 increases by 3.39%, 20.08%, and 30.59%, respectively, compared to the former seam. However, as the number of cleats in the coal seam increases, the incremental gain in peak daily production achieved by extending the cave length diminishes. In Seam #1, when the cavity length is increased from 5 m to 10 m, 15 m, 20 m, 25 m, and 30 m, the peak daily production increases by 11.14%, 17.48%, 22.25%, 25.84%, and 27.20%, respectively. In contrast, in Seam #4, the incremental production increases become 3.45%, 6.88%, 8.98%, 10.92%, and 13.29%. The number of cleats and cavity length in the coal seam have no significant effect on the time to reach peak daily CBM production.

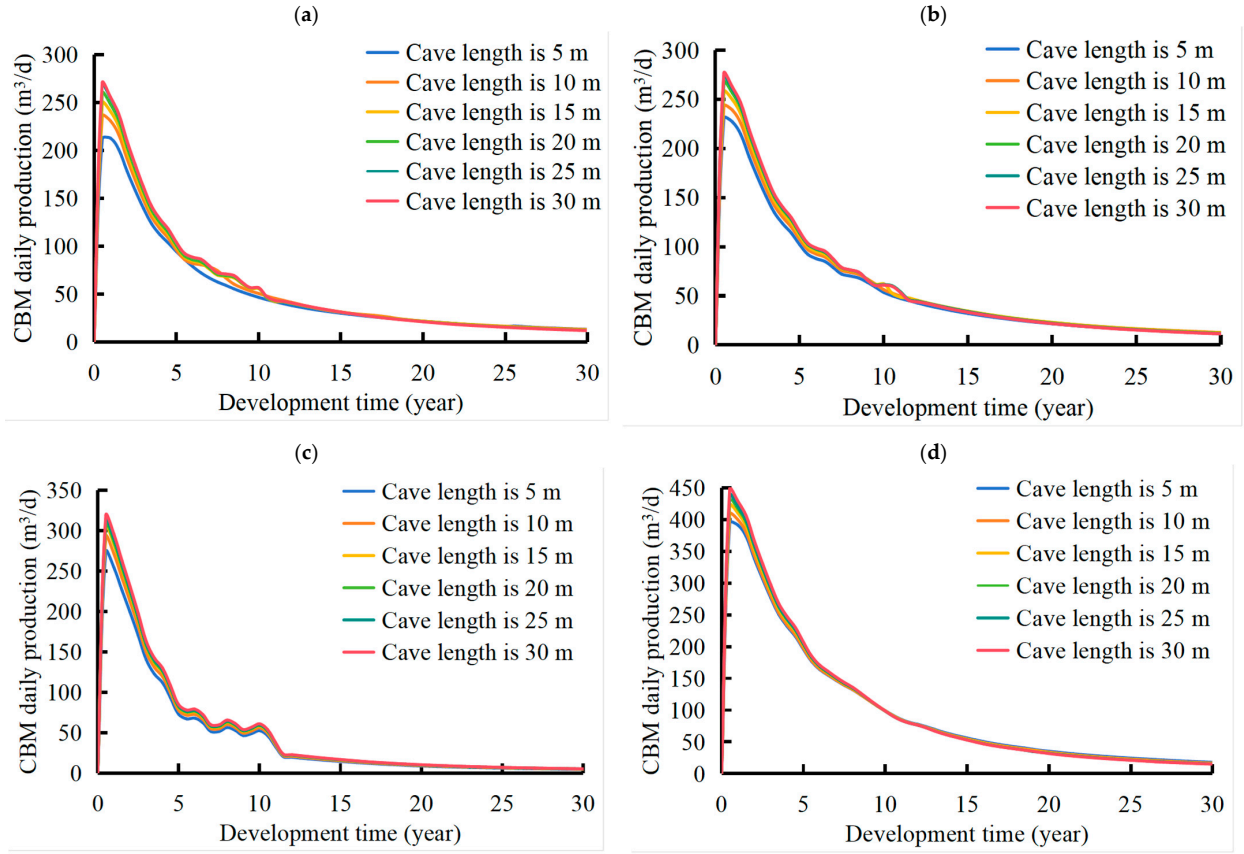


Figure 8. Effects of cave length on productivity in different coal seams: (**a**) Coal seam 1#; (**b**) Coal seam 2#; (**c**) Coal seam 3#; (**d**) Coal seam 4#.

4.4. Effects of Cave Radius on CBM Productivity

Further simulations reveal the impact of cave radius on the daily production of CBM, as illustrated in Figure 9. It can be observed that the effect of cave radius on the peak daily CBM production is similar to that of cave length; as both the cave radius and the number of cleats in the coal seam increase, the peak daily production of CBM continues to rise. However, there is a notable difference: in coal seams with a lower cleat density (Coal seam #1 and Coal seam #2), the influence of cavity radius on peak daily CBM production significantly diminishes once the radius exceeds 1 m.

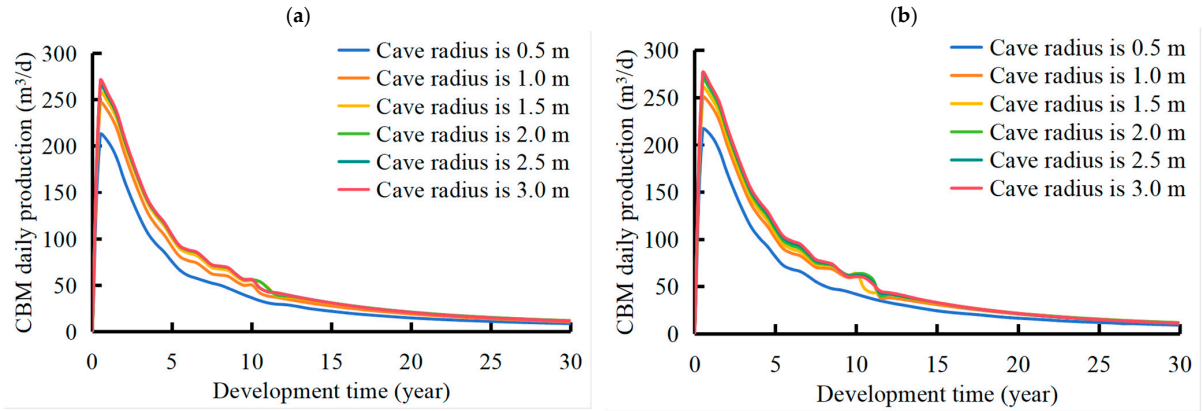


Figure 9. *Cont.*

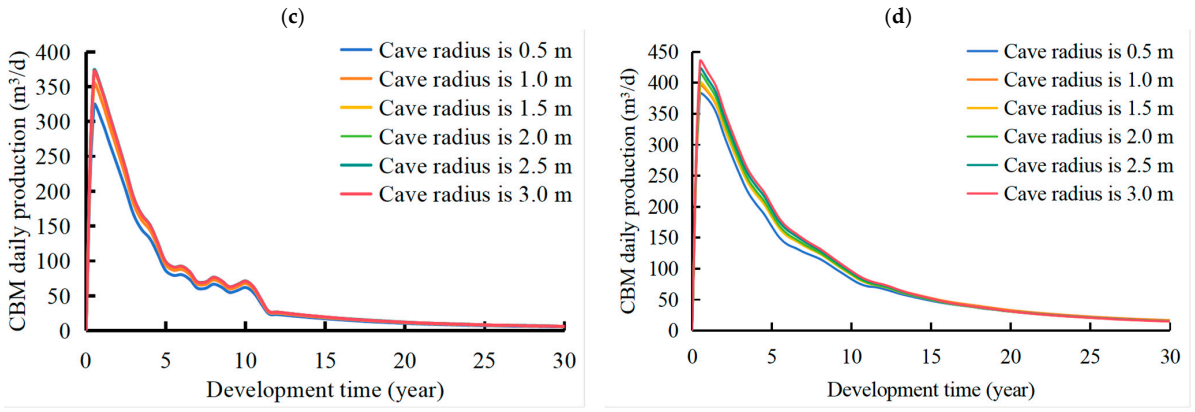


Figure 9. Effects of cave radius on productivity in different coal seams: (**a**) Coal seam 1#; (**b**) Coal seam 2#; (**c**) Coal seam 3#; (**d**) Coal seam 4#.

4.5. CBM Stable Production Time and Cumulative Production

The comparison of the stable production duration, defined as the period during which daily production exceeds 100 m^3/d, for three enhancement methods—hydraulic fracturing, slotting, and cavity creation—is presented in Figure 10, and their cumulative production over a 10–year period is shown in Figure 11. In Coal seam #1, which has a relatively low number of cleats, the stable production periods for hydraulic fracturing and cavity creation are similar. As the cleat numbers increase in Coal seams #2 and #3, the stable production period for hydraulic fracturing reaches approximately 8 years, whereas that for cavity creation is less than 6 years. However, in Coal seam #4, where the cleat number is further increased, the stable production period for cavity creation extends beyond 9 years. Slotting consistently maintains a stable production period of 9–10 years, irrespective of cleat density.

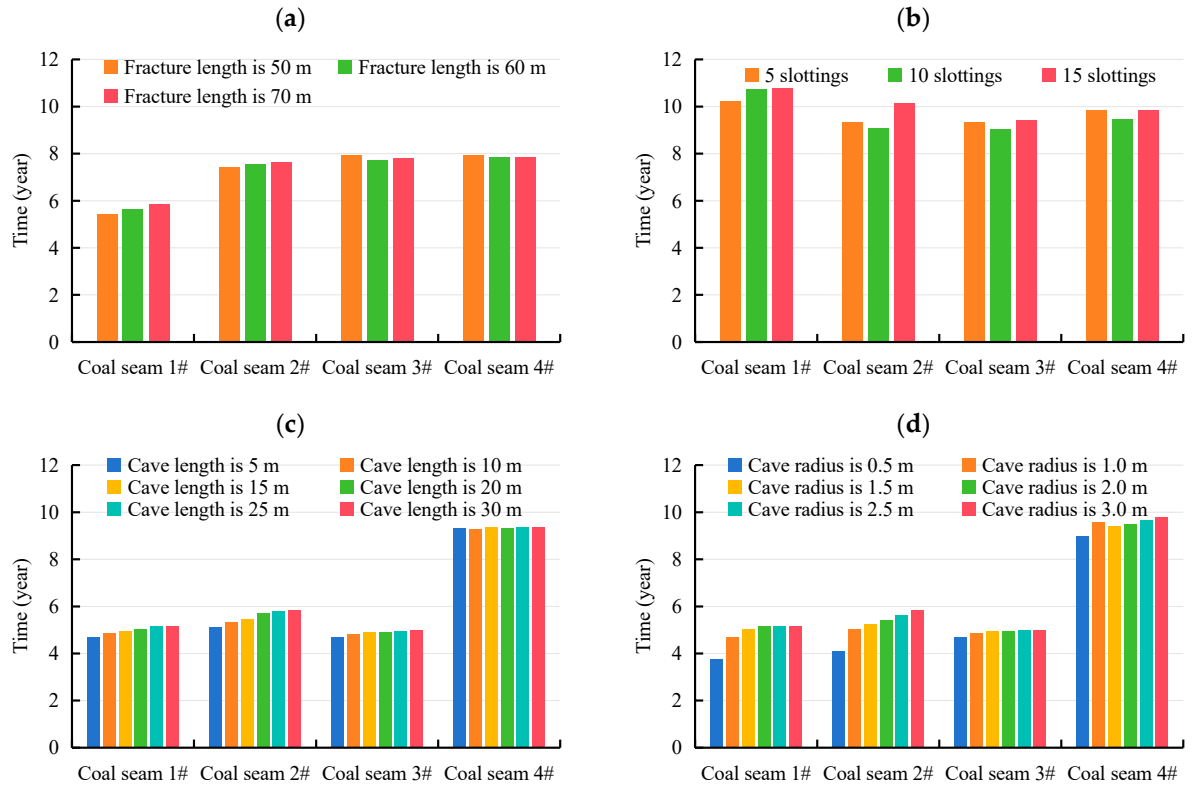


Figure 10. Stable production time of CBM with different stimulation methods: (**a**) Effect of fracture length; (**b**) Effect of slotting number; (**c**) Effect of cave length; (**d**) Effect of cave radius.

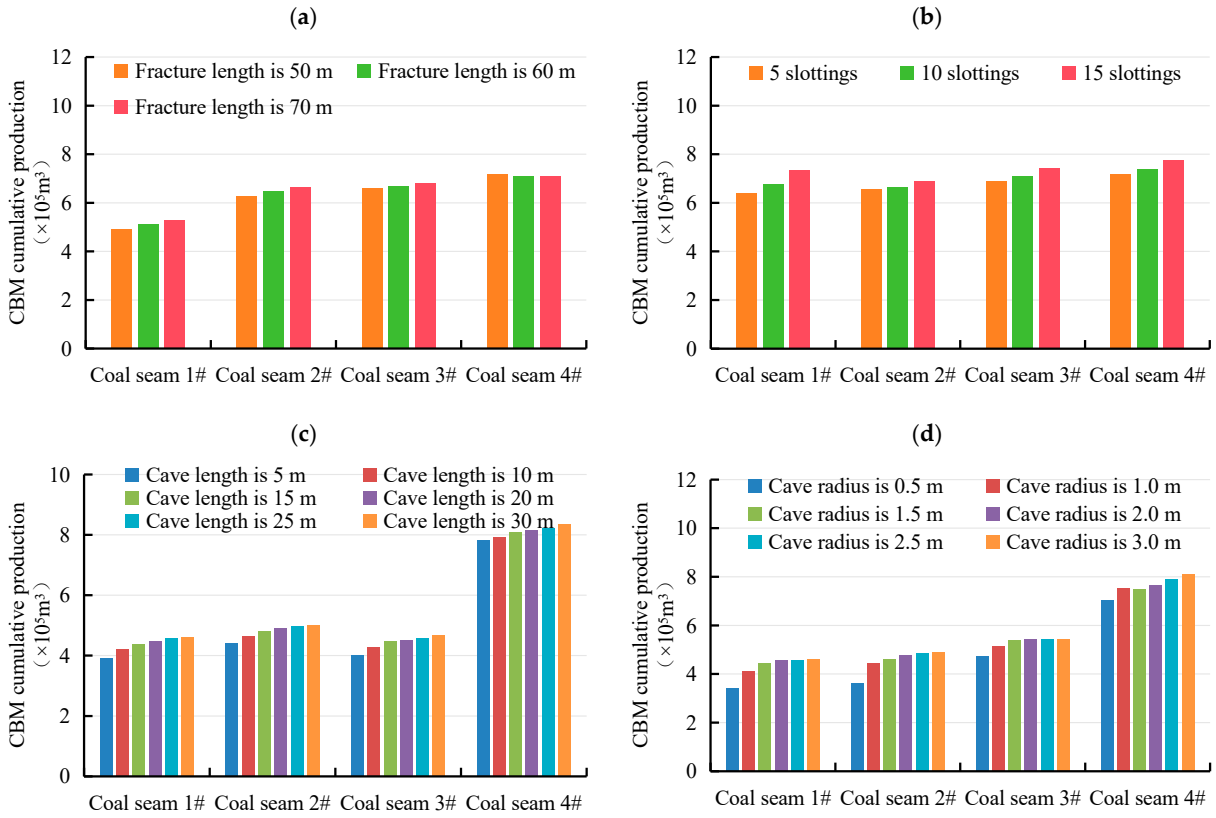


Figure 11. Cumulative production of CBM with different stimulation methods: (**a**) Effect of fracture length; (**b**) Effect of slotting number; (**c**) Effect of cave length; (**d**) Effect of cave radius.

When comparing the cumulative production of CBM, it is evident that in coal seams with varying cleat densities, the cumulative production for hydraulic fracturing and cleating largely falls within the range of 6 to 8 $\times$ 10^5 m^3. In contrast, cavity completion yields a cumulative production of less than 6 $\times$ 10^5 m^3 in Coal seams #1, #2, and #3. Cavity completion achieves a cumulative production of approximately 8 $\times$ 10^5 m^3 only in Coal seam #4, which exhibits the highest cleat density.

5. Conclusions

(1) Both the peak daily production and cumulative production of CBM can be enhanced by increasing the number of slots, as well as by increasing the length of hydraulic fractures and the dimensions (length and radius) of cavities. However, due to the random distribution of cleats within the coal seam, there can be significant variability in the impact of increasing cleat numbers on cumulative production. This is particularly true for the impact on cumulative production by slotting, which appears to be minimal.

(2) Regarding the stable production period for CBM, in coal seams with 19 cleats, slotting results in the longest stable production time, about 10.57 years, followed by hydraulic fracturing, with cavity creation being the least effective, only 4.98 years. Conversely, in coal seams with a higher number of cleats, the stable production periods with cavity creation and slotting have little difference, about 9.47 years, whereas hydraulic fracturing is the least effective, only 7.86 years.

(3) In terms of cumulative production of CBM, in low–cleat coal seams, slotting results in the highest cumulative production, about 68 $\times$ 10^4 m^3, followed closely by hydraulic fracturing, with cavity creation being the least effective, only 43 $\times$ 10^4 m^3. In contrast, in coal seams with a greater number of cleats, cavity creation achieves the highest

cumulative production, reaching 78 × 10^4 m^3, followed by slotting, with hydraulic fracturing being the least effective.

(4) For hydraulic fracturing, this technique is more effective in coal seams with more cleats. In contrast, slotting is not sensitive to the development of cleats within the coal seam and is more effective than hydraulic fracturing regardless of the cleat development level. However, cavity creation is highly sensitive to cleat development; it is suitable for coal seams with well–developed cleats, but its effectiveness is inferior to both hydraulic fracturing and slotting in coal seams where cleats are not well–developed.

Author Contributions: Methodology: H.L. and J.X.; Software: Y.X. and M.W.; Formal analysis: X.Z. (Xueying Zhang); Investigation: W.F. and X.Z. (Xingyuan Zhu). All authors have read and agreed to the published version of the manuscript.

Funding: This research was funded by Basic Research Funds for Universities of Liaoning Provincial Department of Education (No. LJ212410148046), Study on the Enrichment Patterns and Development Mechanisms of Coalbed Methane (No. 2024DJ23), Study on the Enrichment Mechanisms and Pilot Demonstration of Mid– to Low–Rank Coalbed Methane in the Xinjiang Region (No. 2024B03002) and Efficient Development Technologies and Integrated Demonstration for Mid– to Low–Rank Coalbed Methane in the Xinjiang Region (No. 2024ZD140600).

Data Availability Statement: The original contributions presented in this study are included in the article. Further inquiries can be directed to the corresponding author.

Conflicts of Interest: Authors Haibing Lu, Yuhang Xiao, Meizhu Wang and Xueying Zhang were employed by China National Petroleum Corporation. The remaining authors declare that the research was conducted in the absence of any commercial or financial relationships that could be construed as a potential conflict of interest.

References

1. Johnson, R.C.; Flores, R.M. Developmental geology of coalbed methane from shallow to deep in Rocky Mountain basins and in Cook Inlet–Matanuska basin, Alaska, USA and Canada. *Int. J. Coal Geol.* **1998**, *35*, 241–282. [CrossRef]
2. Lau, H.C.; Li, H.; Huang, S. Challenges and opportunities of coalbed methane development in China. *Energy Fuels* **2017**, *31*, 4588–4602. [CrossRef]
3. Li, D.; Gao, X.; Liu, Z.; Zan, X.; Zheng, Z.; Jia, J.; Wu, J. Comparison and revelation of coalbed methane resources distribution characteristics and development status between China and America. *Coal Sci. Technol.* **2018**, *46*, 252–261. Available online: https://www.mtkxjs.com.cn/en/article/id/aa806860-c1b6-4b75-831b-41c5db988ffd (accessed on 10 August 2025).
4. Tao, S.; Chen, S.; Pan, Z. Current status, challenges, and policy suggestions for coalbed methane industry development in China: A review. *Energy Sci. Eng.* **2019**, *7*, 1059–1074. [CrossRef]
5. Qin, Y.; Moore, T.A.; Shen, J.; Yang, Z.; Shen, Y.; Wang, G. Resources and geology of coalbed methane in China: A review. In *Coal Geology of China*; Routledge: London, UK, 2020; pp. 247–282. Available online: https://www.taylorfrancis.com/chapters/edit/10.4324/9780429449369-12/resources-geology-coalbed-methane-china-review-yong-qin-tim-moore-jian-shen-zhaobiao-yang-yulin-shen-geoff-wang (accessed on 9 August 2025).
6. Ma, H.; Yang, Y.; Xue, Z.; Clarkson, C.R.; Chen, Z. Transitioning from emission source to sink: Economic and environmental trade-offs for CO_2-enhanced coalbed methane recovery of Mannville coal Canada. *Sci. Total Environ.* **2025**, *966*, 178721. [CrossRef] [PubMed]
7. Prabu, V.; Mallick, N. Coalbed methane with CO_2 sequestration: An emerging clean coal technology in India. *Renew. Sustain. Energy Rev.* **2015**, *50*, 229–244. [CrossRef]
8. Pan, Z.; Ye, J.; Zhou, F.; Tan, Y.; Connell, L.D.; Fan, J. CO_2 storage in coal to enhance coalbed methane recovery: A review of field experiments in China. *Coal Geol. China* **2020**, 224–246. [CrossRef]
9. Khoshmagham, A.; Hosseini Alaee, N.; Shirinabadi, R.; Bangian Tabrizi, A.H.; Gholinejad, M.; Kianoush, P. Geological Characteristics of Coal Mines in the Zagros Basin of Iran: Unveiling Rock Mechanical Properties and Time-Dependent Behavior. *Energy Geosci.* **2025**, *6*, 100361. [CrossRef]
10. Tambaria, T.N.; Sugai, Y.; Nguele, R. Adsorption factors in enhanced coal bed methane recovery: A review. *Gases* **2022**, *2*, 1–21. [CrossRef]
11. Zhou, F.; Liu, S.; Pang, Y.; Li, J.; Xin, H. Effects of coal functional groups on adsorption microheat of coal bed methane. *Energy Fuels* **2015**, *29*, 1550–1557. [CrossRef]

12. Liu, X.; He, X. Effect of pore characteristics on coalbed methane adsorption in middle-high rank coals. *Adsorption* **2017**, *23*, 3–12. [CrossRef]
13. Liu, X.; Song, D.; He, X.; Nie, B.; Wang, Q.; Sun, R.; Sun, D. Coal macromolecular structural characteristic and its influence on coalbed methane adsorption. *Fuel* **2018**, *222*, 687–694. [CrossRef]
14. Lv, F.; Yang, R.; Gao, W.; Zhao, L.; Liu, Y.; Yan, Z.; Shi, F.; Zhang, B.; Tang, J.; Yi, T. Critical depth prediction based on in–situ stress and gas content model of deep coalbed methane in Liupanshui Coalfield in China. *Sci. Rep.* **2025**, *15*, 297. [CrossRef]
15. Liu, S.; Fan, K.; Jin, Y.; Yu, Z.; Dong, J.; Wang, C. Stress sensitivity characteristics of deep coal reservoirs and its influence on coalbed methane productivity. *Coal Geol. Explor.* **2022**, *50*, 56–64. [CrossRef]
16. Liu, S.; Wang, J.; Wu, J.; Tang, Y. Modification and enhancement of permeability of coal seam using mined CO_2 foam fracturing fluid. *J. Nat. Gas Sci. Eng.* **2018**, *60*, 32–39. [CrossRef]
17. Huang, Q.; Li, M.; Li, J.; Gui, Z.; Du, F. Comparative experimental study on the effects of water-and foam-based fracturing fluids on multiscale flow in coalbed methane. *J. Nat. Gas Sci. Eng.* **2022**, *103*, 104648. [CrossRef]
18. Xu, J.; Zhai, C.; Qin, L. Mechanism and application of pulse hydraulic fracturing in improving drainage of coalbed methane. *J. Nat. Gas Sci. Eng.* **2017**, *40*, 79–90. [CrossRef]
19. Zhou, F.; Chen, Z.; Rahman, S.S. Effect of hydraulic fracture extension into sandstone on coalbed methane production. *J. Nat. Gas Sci. Eng.* **2015**, *22*, 459–467. [CrossRef]
20. Li, Q.; Li, Q.; Wang, F.; Ning, X.; Wang, Y.; Bai, B. Settling behavior and mechanism analysis of kaolinite as a fracture proppant of hydrocarbon reservoirs in CO_2 fracturing fluid. *Colloids Surf. A Physicochem. Eng. Asp.* **2025**, *724*, 137463. [CrossRef]
21. Li, Q. Reservoir Science: A Multi-Coupling Communication Platform to Promote Energy Transformation, Climate Change and Environmental Protection. *Reserv. Sci.* **2025**, *1*, 1–2. [CrossRef]
22. Hao, C.; Cheng, Y.; Wang, L.; Liu, H.; Shang, Z. A novel technology for enhancing coalbed methane extraction: Hydraulic cavitating assisted fracturing. *J. Nat. Gas Sci. Eng.* **2019**, *72*, 103040. [CrossRef]
23. Li, H.; Cao, Y.; Zhou, D.; Chai, X.; Liu, T.; Feng, P.; Shi, B.; Tian, L. Fracturing parameters analysis and productivity evaluation of vertical coalbed methane wells with nitrogen foam. *Coal Geol. Explor.* **2020**, *48*, 11. [CrossRef]
24. Zhang, J. Numerical simulation of hydraulic fracturing coalbed methane reservoir. *Fuel* **2014**, *136*, 57–61. [CrossRef]
25. Jiang, T.; Zhang, J.; Wu, H. Effects of fractures on the well production in a coalbed methane reservoir. *Arab. J. Geosci.* **2017**, *10*, 494. [CrossRef]
26. Zhu, J.; Tang, J.; Hou, C.; Shao, T.; Zhao, Y.; Wang, J.; Lin, L.; Liu, J.; Jiang, Y. Two-phase flow model of coalbed methane extraction with different permeability evolutions for hydraulic fractures and coal reservoirs. *Energy Fuels* **2021**, *35*, 9278–9293. [CrossRef]
27. Chen, Z.; Sun, T. Evaluation Method of Coal-Bed Methane Fracturing in the Qinshui Basin. *Math. Probl. Eng.* **2020**, *2020*, 1545729. [CrossRef]
28. Yang, R.; Chen, J.; Qin, X.; Huang, Z.; Li, G.; Liu, L. Stress evolution and permeability enhancement mechanism of multistage cavity completion in coalbed methane horizontal wells. *SPE J.* **2023**, *28*, 2767–2789. [CrossRef]
29. Zhong, J.; Ge, Z.; Lu, Y.; Zhou, Z.; Zheng, J. New mechanical model of slotting–directional hydraulic fracturing and experimental study for coalbed methane development. *Nat. Resour. Res.* **2021**, *30*, 639–656. [CrossRef]
30. Yang, R.; Huang, Z.; Li, G.; Sepehrnoori, K.; Li, K. Slotted Liner Sheathing Coiled Tubing Fishbone Jet Drilling: An Efficient Approach for Coalbed Methane Recovery. In Proceedings of the International Petroleum Technology Conference (IPTC), Bangkok, Thailand, 14–16 November 2016. IPTC-18893-MS. [CrossRef]
31. Holditch, S.A. Completion methods in coal-seam reservoirs. *J. Pet. Technol.* **1993**, *45*, 270–276. [CrossRef]
32. Palmer, I.D.; Mavor, M.J.; Seidle, J.P.; Spitler, J.L.; Voiz, R.F. Openhole cavity completions in coalbed methane wells in the San Juan Basin. *J. Pet. Technol.* **1993**, *45*, 1072–1080. [CrossRef]
33. Palmer, I. Coalbed Coalbed methane completions: A world view. *Int. J. Coal. Geol.* **2010**, *82*, 184–195. [CrossRef]
34. Shi, J.Q.; Durucan, S.; Sinka, I.C. Key parameters controlling coalbed methane cavity well performance. *Int. J. Coal Geol.* **2002**, *49*, 19–31. [CrossRef]
35. Wei, G.; Wen, H.; Deng, J.; Li, Z.; Fan, S.; Lei, C.; Liu, M.; Ren, L. Enhanced coalbed permeability and methane recovery via hydraulic slotting combined with liquid CO_2 injection. *Process Saf. Environ. Prot.* **2021**, *147*, 234–244. [CrossRef]
36. Lin, B.; Yan, F.; Zhu, C.; Zhou, Y.; Zou, Q.; Guo, C.; Liu, T. Cross-borehole hydraulic slotting technique for preventing and controlling coal and gas outbursts during coal roadway excavation. *J. Nat. Gas Sci. Eng.* **2015**, *26*, 518–525. [CrossRef]
37. Si, G.; Durucan, S.; Shi, J.Q.; Korre, A.; Cao, W. Parametric analysis of slotting operation induced failure zones to stimulate low permeability coal seams. *Rock Mech. Rock Eng.* **2019**, *52*, 163–182. [CrossRef]
38. Cheng, S.; Li, Q.; Zhou, Y.; Xia, B.; Gong, T.; Yang, J.; Zhang, Y. Stress relief cracking and permeability improvement by high-pressure water jet slotting to enhance coalbed methane extraction. *Pet. Sci. Technol.* **2025**, *43*, 1444–1465. [CrossRef]
39. Qin, L.; Li, J.; Mu, M.; Lv, S.; Chen, N.; Xiong, M. Impact of controllable parameters in hydraulic slotting on stress relief effects around coal seam. *Phys. Fluids* **2025**, *37*, 037105. [CrossRef]

40. Zhen, H.; Zhao, H.; Wei, K.; Liu, Y.; Li, S.; Wei, Z.; Wang, C.; Chen, G. Innovative Stress Release Stimulation Through Sequential Cavity Completion for CBM Reservoir Enhancement. *Processes* **2025**, *13*, 1567. [CrossRef]
41. Geng, Y.L.; Qi, X.Y.; Jia, S.P. Gas-solid Coupling Model by Considering Desorption Effect. *J. Hunan Univ. Sci. Technol. Nat. Sci. Ed.* **2020**, *35*, 40–48. [CrossRef]
42. Tao, S.; Pan, Z.; Tang, S.; Chen, S. Current status and geological conditions for the applicability of CBM drilling technologies in China: A review. *Int. J. Coal Geol.* **2019**, *202*, 95–108. [CrossRef]
43. Beaton, A.; Langenberg, W.; Pană, C. Coalbed methane resources and reservoir characteristics from the Alberta Plains, Canada. *Int. J. Coal Geol.* **2006**, *65*, 93–113. [CrossRef]
44. Liu, J.; Chen, Z.; Elsworth, D.; Qu, H.; Chen, D. Interactions of multiple processes during CBM extraction: A critical review. *Int. J. Coal Geol.* **2011**, *87*, 175–189. [CrossRef]

Disclaimer/Publisher's Note: The statements, opinions and data contained in all publications are solely those of the individual author(s) and contributor(s) and not of MDPI and/or the editor(s). MDPI and/or the editor(s) disclaim responsibility for any injury to people or property resulting from any ideas, methods, instructions or products referred to in the content.